Effect of steric crowding on ion selectivity for calix-crown hybrid ionophores: experimental, molecular modeling and crystallographic studies†

Subrata Patra, Debdeep Maity, Anik Sen, E. Suresh, Bishwajit Ganguly* and Parimal Paul*

Received (in Gainesville, FL, USA) 22nd October 2009, Accepted 21st June 2010
DOI: 10.1039/b9nj00587k

A number of calix[4]arene-azacrowns with variation in ring size and substituents at the upper and lower rims have been synthesized to investigate the effect of steric crowding towards ion selectivity. The structural elucidation of these ionophores has been carried out mainly by ^{1}H NMR and ES-MS in solution and by single crystal X-ray study in the solid state. Interaction of these ionophores with a large number of cations has been investigated by NMR studies. The ionophore with *tert*-butyl at the upper rim (**3**) exhibits selectivity towards Na^+ only whereas an ionophore of the same size but without *tert*-butyl at the upper rim (**1**) shows selectivity towards both Na^+ and K^+. An ionophore of the same size but with three tosyl substituents at the lower rim (**4**) exhibits no complexation with any cation. The ionophore with the larger crown ring and without *tert*-butyl at the upper rim (**2**) exhibits complexation with K^+, Rb^+, Ba^{2+} and weak interaction with Na^+. Binding constants with these metal ions have been determined by NMR titration. Molecular modeling studies performed by a molecular mechanics force field (MMFF94) using the Monte Carlo search method and DFT calculations predicted the observed higher selectivity for sterically crowded receptor.

Introduction

Calixarenes, cyclic oligomers made up of phenol units linked by a methylene bridge, are receiving increasing attention because of their potential use as hosts for sensing various analytes.[1–5] In the calixarene family, calix[4]arenes are the most popular because of their rigid structures, which make them ideal candidates for complexation with various ions.[6–9] This chemistry has become more versatile because of the ease with which calix[4]arene can be modified with functional groups at lower and upper rims, depending on the requirement. These modified calixarenes provide a highly preorganized architecture for the assembling of converging binding sites.[10–14] Among calixarene derivatives, calix[4]arene-crown hybrid molecules have attracted intense interest because of their remarkable selectivity towards alkali and alkaline earth metal ions.[15–22] The ion selectivity of this class of compounds is controlled mainly by the conformation of the calixarene platform, the size of the crown ring and the substituents at the upper and lower rims of the calixarene unit. Incorporation of the substituents at the –OH groups of the lower rim suppresses hydrogen-bonding and increases steric hindrance, which results in the formation of conformational isomers such as cone, partial-cone, 1,3-alternate and 1,2-alternate.[15,23–28] In the cone conformation, the appended functional groups at the two sides of the crown ring and in the 1,3-alternate conformation the substituents attached to the crown moiety play an important role to determine selectivity.[8,16,19,21,22] Among various size of crown rings, crown-5 and crown-6 containing calixarene derivatives are found to be more suitable for complexation with alkali-metal ions.[15,18,21,22]

Another class of calix-crown based receptors, in which a nitrogen atom is incorporated in the crown ring has been developed. The presence of a nitrogen atom in the crown ring provides an advantage for attaching desired substituents for a specific study - inclusion of photoactive substituents produced a new class of luminescent molecular sensor and it has been widely used to monitor ion recognition events.[16,22,29–32] Apart from luminescence output, the substituents also play an important role in the determination of selectivity, *e.g.* *N*-chromogenic calix[4]arene azacrown, in which a 2-hydroxy-5-nitrobenzyl group attached on nitrogen, exhibited high potassium selectivity over other metal ions and it was assumed that the OH of the chromogenic group assisted the complexation by encapsulating the metal ion.[16] Another series of calix[4]arene azacrown ethers has been reported in which 2-picolyl, 3-picolyl and benzyl groups were attached on the nitrogen atom and among these compounds, the 2-picolyl armed calixazacrown ether showed the highest selectivity towards silver ions due to electrostatic interactions by encapsulation of the metal ion assisted by the nitrogen atom of the 2-picolyl group.[29] When pyrene was attached to

Analytical Science Division, Central Salt and Marine Chemicals Research Institute (constituents of CSIR, New Delhi), G. B. Marg, Bhavnagar 364 002, India. E-mail: ppaul@csmcri.org, ganguly@csmcri.org; Fax: +91 278 256 7562; Tel: +91-278-2567760

† Electronic supplementary information (ESI) available: H-bonding table (Table S1), packing diagrams of **3** and **4** (Fig. S1 and S2), lowest energy conformer of **4** with Na^+ and K^+ (Fig. S3). CCDC reference numbers 749549–749552. For ESI and crystallographic data in CIF or other electronic format see DOI: 10.1039/b9nj00587k

the nitrogen atom of a similar system it exhibited selectivity towards Cu^{2+}, Pb^{2+}, K^+ and Rb^+, but when the crown ether was incorporated at the upper rim of the calix as a secondary binding site, "molecular taekwondo" processes between Ag^+–K^+, Cu^{2+}–K^+ and Ag^+–Cs^+ were noted.[30,31] In such studies, electrostatic and allosteric effects have been observed to play a role in the selectivity of incoming metal ion(s). However, the effect of steric crowding on ion-selectivity for calix[4]arene azacrown systems has been less explored. The attachment of a non-photoactive substituent, which has the remote possibility to assist encapsulation of a metal ion by interaction, is probably the best way to study the effect of steric crowding on the selectivity of the calix-crown hybrid ionophore.

With an aim to study the effect of bulky substituents on the selectivity of the ionophore, we have synthesized four calix[4]-arene-azacrown compounds with different substituents at the upper and lower rims and also with variation in ring size of the crown moiety. The substituent, *p*-toluene sulfonamide is attached to the nitrogen atom(s) of the crown moiety and *tert*-butyl/hydrogen is incorporated in the upper rim. All of these compounds have been characterized on the basis of analytical and spectroscopic methods and molecular structures have been established by single crystal X-ray studies. A molecular modeling study has been carried out to examine the ion selectivity of these ionophores. The experimental ion selectivity and binding constants with strongly interacting cations have been determined by ^{1}H NMR study. These studies have enabled us to unravel the influence of bulky substituents on the ion-binding property of these ionophores.

Results and discussion

Synthesis and characterization of the ionophores 1–4

The methods followed for the synthesis of **1–4** are shown in Scheme 1 and details of experimental procedures are given in the experimental section. Elemental analysis (C, H, N and S), ^{1}H NMR and mass spectrometric data of **1–4** and for some of the intermediates are given in the experimental section. The elemental analysis and mass data are in excellent agreement with the calculated values. It may be noted that *e*/*m* values of all these compounds correspond to the $Na^+/K^+/H^+$ adduct, which is a well known phenomenon when LC-MS is used for the measurement of mass.[21,22,25,33] The ^{1}H NMR spectral data are consistent with the structures shown in Scheme 1. The appearance of ArCH_2Ar methylene protons as a multiplet in the region δ 3.60–3.90 confirmed the 1,3-alternate conformation of these compounds in solution.[18,34] The methyl group of the tosyl moiety appears as a singlet for **1–3** at δ 2.45, however for **4** it appears as two closely spaced singlets at δ 2.47 (6H) and 2.49 (3H), indicating that two of the three methyl groups are chemically equivalent and the third one is slightly different.

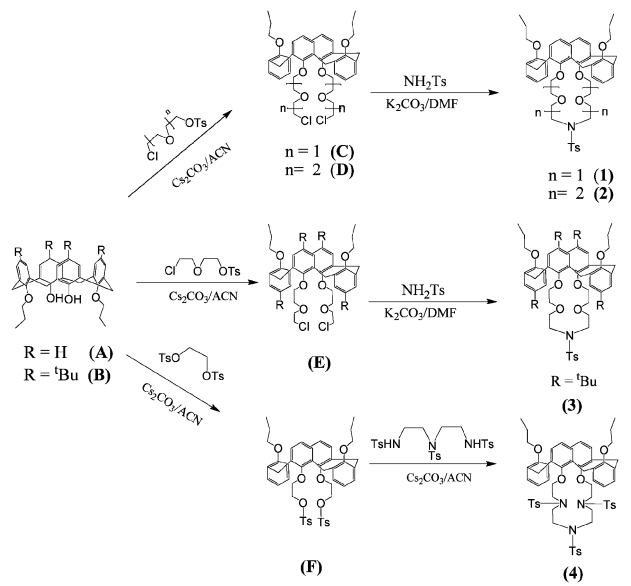

Scheme 1 Synthetic route for compounds **1–4**.

Crystal structures of 1–4

The ORTEP diagrams of **1–4** of one of the molecules present in the asymmetric unit with atom numbering scheme are shown in Fig. 1. Details of the experimental procedure and crystallographic data are presented in the experimental section. For all of the four compounds, bond lengths and bond angles are in the usual ranges,[10,11,15,21,25] and the following discussion refers mainly to the conformation and shape of the calixarene skeleton. Crystal structures clearly show that all of these compounds have adopted the 1,3-alternate conformation with the two propyl groups at

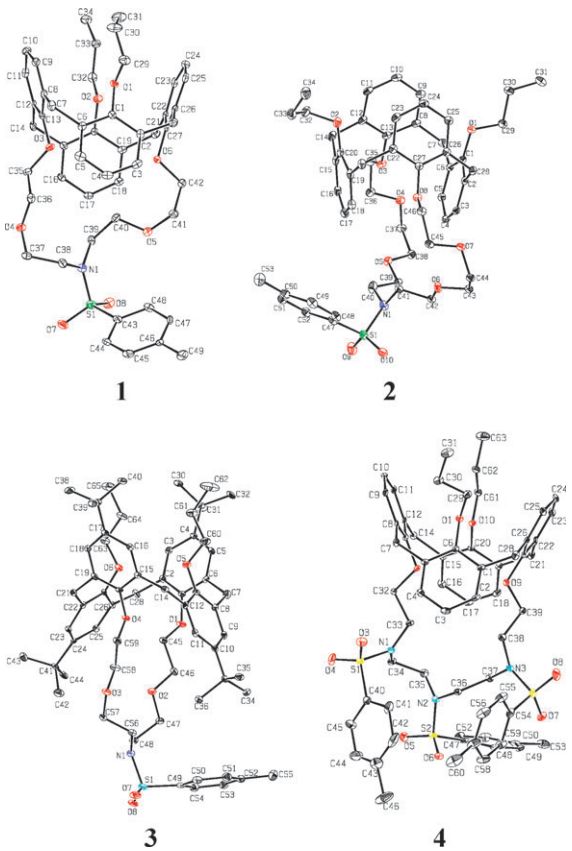

Fig. 1 ORTEP views of the compounds **1–4** with atom numbering scheme (30% probability factor for the thermal ellipsoids).

the upper rim; however the precise shape of the molecule differs due to variation in substituents. In 1,3-alternate arrangements, the dihedral angles between the four phenyl rings and the mean plane of the methylene groups varies significantly (51.97°–81.51°) because of the presence of different substituents at the upper and lower rims.

To understand the arrangement of the molecules in the crystal lattice, the hydrogen bonding interaction and packing pattern have been analyzed in detail. All four compounds exhibited a number of strong intermolecular H-bonding interactions, however the types of interactions are distinctly different from compound to compound. A brief description of these interactions is given below and the H-bonding parameters are summarized in Table S1 (in the ESI†).

In compound **1**, the two molecules (molecules 1 and 2) present in the asymmetric unit and associated *via* C–H···O interactions generating two independent layers of helical hydrogen bonded networks *via* 2_1 screw related adjacent molecules along the *bc*-plane as depicted in Fig. 2. The ether oxygen O4 of molecule 1 is involved in a C–H···O interaction with the phenyl hydrogen atom H45 of the adjacent molecule 1 of the tosyl group; while in the case of molecule 2, the sulfonate oxygen O16 of the tosyl group makes a C–H···O interaction with the phenyl hydrogen H66 of the calix moiety forming a layered helical network. For compound **2**, the two molecules in the asymmetric unit are associated like compound **1** *via* C–H···O interactions; however the pattern of H-bonding is different. In molecule 1, the sulfonate oxygen O9 and the phenyl hydrogen H25 of the calix moiety interact, generating a hydrogen-bonded strand along the *a*-axis. Molecule 2 present in the asymmetric unit is oriented along with the H-bonded strand of molecule 1 in such a way that the sulfonate groups of molecule 1 (O10) and 2 (O20) are sufficiently close to make effective C–H···O interactions with phenyl hydrogen atoms H101 and H45, respectively, generating the hydrogen bonded layers as shown in Fig. 3.

For **3**, the adjacent calix moieties are oriented in opposite directions as a layer along the *b*-axis involving a C–H···O interaction between the phenolic oxygen of the calix with the *tert*-butyl hydrogen H43 of the neighbouring molecule. These layers are further cross-linked *via* a C–H···O interaction between the sulfonate oxygen O7 of the tosyl group from either side of the oppositely oriented H-bonded calix layers with phenyl hydrogen H11 and form two-dimensional sheets

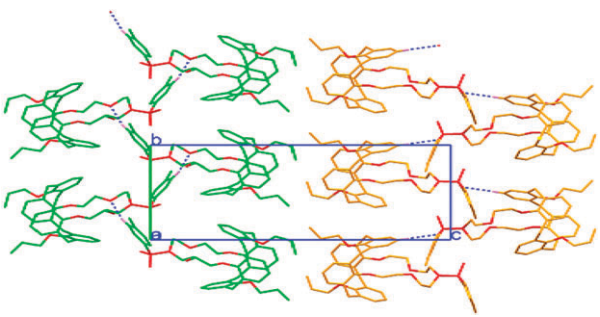

Fig. 2 Packing diagram of compound **1** viewed down the *a*-axis showing the hydrogen bonded layered helical network between the screw related molecules present in the asymmetric unit.

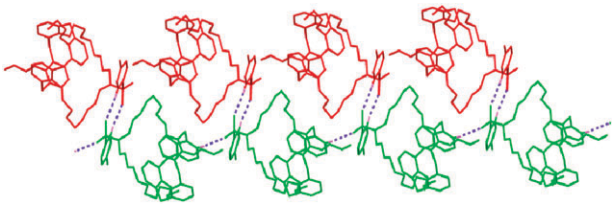

Fig. 3 Packing diagram of compound **2** depicting the close-up view of the hydrogen bonding interaction (dotted blue line) between the two molecules present in the asymmetric unit.

(see Fig. S1 in the ESI†). For compound **4**, the adjacent molecules are oriented in opposite directions and associated *via* a C–H···O interaction between the sulfonate oxygen O8 and phenyl hydrogen H25 of the calix moiety in dimeric association. These hydrogen bonded dimers are oriented almost diagonally to the *ac* plane (see Fig. S2 in the ESI†). It is also interesting to note that the phenyl hydrogen H18 of the calix moiety is involved in intermolecular C–H···π interactions with the phenyl ring C8–C13 [C(18)–H(18)···Cg(2): H(18)···Cg(2) = 2.75 Å, C18···Cg(2) = 3.672(6) Å, ∠C(18)–H(18)···Cg(2) = 78°, symmetry code: $1 - x, -1/2 + y, 1/2 - z$, where Cg(2) is the center of gravity of the phenyl ring (C8–C13)].

Ion binding study

The cation-binding ability of the ionophores **1–4** has been studied by ^{1}H NMR using a number of metal ions Li^+, Na^+, K^+, Rb^+, Cs^+, Mg^{2+}, Ca^{2+}, Sr^{2+}, Ba^{2+}, Zn^{2+}, Cd^{2+}, Hg^{2+} and Pb^{2+}. The ^{1}H NMR spectra of all four complexes were recorded in the presence of 100 fold excess of the above-mentioned metal ions and these spectra were compared with the absence of a metal ion to ascertain the complexation behaviour of the ionophores. For compounds **1–3**, significant changes in the ^{1}H NMR spectra were noted in the presence of certain metal ions, whereas compound **4** did not show any change with all of these metal ions. The spectral changes observed with Na^+ and K^+ for **1**, Na^+, K^+, Rb^+ and Ba^{2+} for **2**, and with only Na^+ for **3**, indicated complexation of these metal ions with the respective ionophores.

Complexation with various metal ions was also confirmed by mass spectrometry. The ionophore and the desired metal ion were mixed in an appropriate solvent and stirred at room temperature, as described in the experimental section, and the mass spectrum of the resultant solution was recorded. The mass data, given in the experimental section, are in excellent agreement with the 1 : 1 complex formation.

For the determination of binding constants, NMR titrations were carried out with the above-mentioned metal ions. Interestingly, in the case of K^+ for **1**, and Na^+ for **3**, upon addition of increasing concentrations of metal ions new peaks were observed with a gradual disappearance of the original signals as shown in Fig. 4. In all other cases, a gradual shift of certain signals was noted with the addition of metal ions. The changes were observed in the aliphatic region for signals due to the crown moiety because of its involvement in coordination with the metal ion. However, changes in chemical shifts of some other signals were also noted due to conformational changes

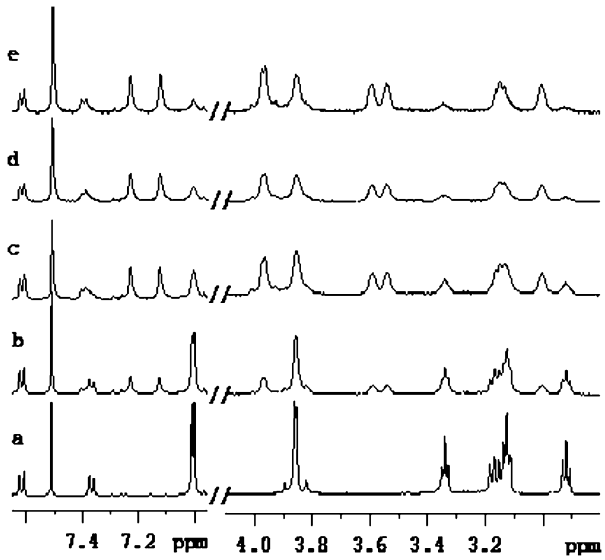

Fig. 4 Selected portion of the ^{1}H NMR spectra for **3** upon addition of 0.0 (a), 0.5 (b), 1.0 (c), 4.0 (d) and 8.0 (e) molar equivalent amounts of $NaClO_4$; new peaks are growing with the disappearance of the peaks of the original complex.

induced by metal coordination. Upon addition of the metal ions, growth of new signals with the disappearance of original one indicates formation of a stable complex, *i.e.* the rate of decomplexation is too slow in NMR time scale. This is due to the fact that 1,3-alternatecalix[4]-arenes are conformationally rigid and if the size of the cavity containing π–electron clouds in the distal phenyl units is close to the size of the ionic diameter then strong binding of metal ions takes place.[35,36] However, if the sizes of metal ions are not large enough compared to the cavity size to cause cation–π interaction with the π–electron clouds, then weak complexation takes place. In this case, the rate of decomplexation is fast enough in NMR time scale for an average of chemical shifts due to complexed and uncomplexed species, and a shift in the NMR signal can be observed. In the case of **2**, which has a large cavity size, the metal ions (Na^+, K^+, Rb^+ and Ba^{2+}) are not big enough to make strong conformationally rigid complexes using π-electron clouds in the distal phenyl units. The cavity size of the crown moiety of **1** and **3** should be appropriate for K^+, however the latter did not show complexation with K^+. Possibly the steric effect due to bulky *tert*-butyl groups from both sides in 1,3-alternate conformation prevents K^+ entering into the cavity for complexation. In the case of shifting of the signals, the extent of the shift with respect to the limiting value corresponds to the concentration of the complex formed. Fig. 5 shows the changes in chemical shifts of certain signals for complex **2** upon addition of Ba^{2+}. The changes observed in the region δ 3.35–3.65 are due to the coordination of Ba^{2+} with the crown moiety, whereas the changes in chemical shifts for some other signals of the calix unit are due to the metal induced conformational change of the molecule as a whole.

Binding constants for the systems, where chemical shifts gradually changed upon addition of increasing metal ion concentration (Na^+ for **1**, and Na^+, K^+, Rb^+ and Ba^{2+} for **2**), were calculated using the program developed by

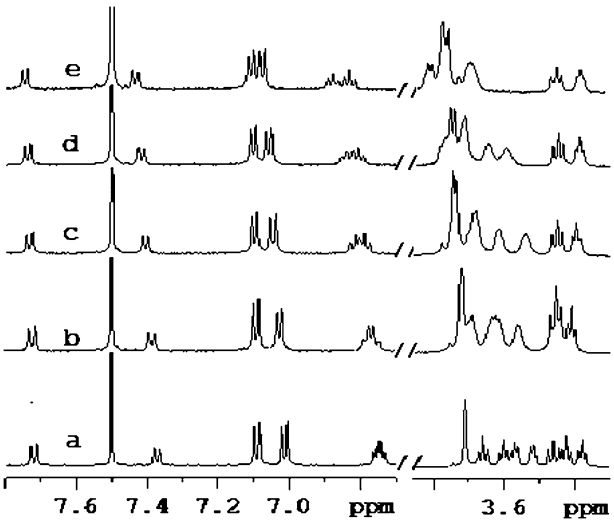

Fig. 5 Selected portion of the ^{1}H NMR spectra for **2** upon addition of 0.0 (a), 1.0 (b), 2.0 (c), 4.0 (d) and 10.0 (e) molar equivalent amounts of $Ba(ClO_4)_2$; chemical shifts of certain signals change with increasing concentration of the metal ion.

Table 1 Binding constants (K_s) for the ionophores **1–3**

Ionophore	Metal ion	Binding constant (K_s/M^{-1})
1	Na^+	3.10×10^3
	K^+	4.17×10^3
2	Na^+	6.00×10
	K^+	4.19×10^3
	Rb^+	4.55×10^4
	Ba^{2+}	3.35×10^2
3	Na^+	2.05×10^3

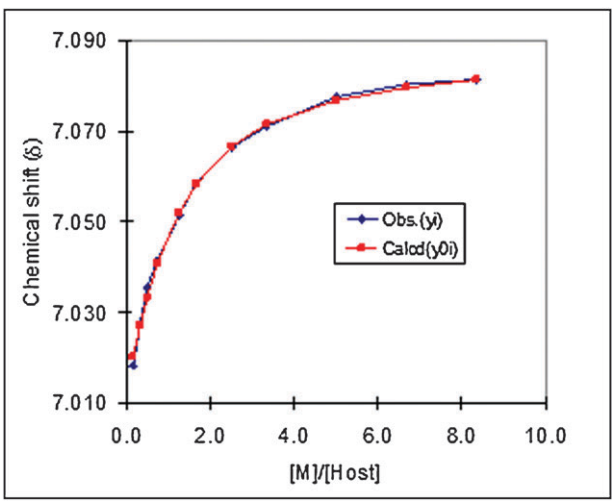

Fig. 6 The non-linear least square fit from ^{1}H NMR titration data for the determination of binding constant for **2** with Ba^{2+} in CD_3CN-$CDCl_3$ (3 : 1) at room temperature.

Hirose[37] and the data are given in Table 1. The non-linear least square fit for **2** with Ba^{2+} is shown in Fig. 6. For the systems, where new peaks have grown, the binding constants were determined by direct method using peak intensity ratio.[22,24,38] Summation of the intensities of both the peaks

corresponds to the initial (total) concentration of the complex, the intensity ratio of the growing peak corresponds to the concentration of the cation-bound complex and the intensity ratio of the disappearing peak corresponds to the concentration of the remaining complex (without cation-binding). Binding constant (K_s) was then calculated using the equation $K_s = [C]/([H_t] - [C])([G_t] - [C])$, where [C] is the concentration of the cation-bound complex, $[H_t]$ is the total concentration of the host (complex) and $[G_t]$ is the total concentration of the guest metal ion.[37] Measurements were carried out with four different concentrations of complex and also K_s values with a 20% to 80% complexation ratio were considered to minimize error in measurement.[37] The K_s values from NMR measurement are summarized in Table 1 and the data suggest moderate to strong complexation of the ionophores with the metal ions. For compound **2**, the binding constants are in the order $60 < 6.14 \times 10^2 < 4.19 \times 10^3 < 4.54 \times 10^4$ for Na^+, Ba^{2+}, K^+ and Rb^+, respectively, the highest value is for the metal ion (Rb^+) having the largest ionic diameter (2.94 Å) among the cations studied (K^+ = 2.66 Å, Ba^{2+} = 2.68 Å). For **1**, the binding constant of K^+ is slightly higher than that of Na^+. It may be noted that the size of the ionophores (azacrown ring) and substituent at the azacrown ring for **1** and **3** are the same but they exhibit remarkably different ion selectivity due to steric crowding imposed by the *tert*-butyl group attached to **3**. The ring size of **4** is similar to that of **1**, but the former has three tosyl substituents at the azacrown ring and did not form a complex with any metal ion studied here. Therefore, the results indicate that steric crowding plays an important role in determining ion selectivity in these systems.

Comparison of the ion-selectivity and binding constants observed in the present study with the reported similar calix[4]arene azacrown-5/6 ionophores is not straightforward. The reason is that in most of the cases the moiety attached on the nitrogen atom of the azacrown ring assists encapsulation of the metal ion in the crown cavity through interaction.[16,29] Therefore, the ion-binding property of these systems cannot be compared with the systems where only steric effect governs the selectivity of metal ions. In some cases the attached group, *e.g.* benzyl unit, did not make any interaction with the metal ion but an ion-binding study was carried out by two-phase extraction using a picrate anion.[29] It is well known that picrate forms a strong ion-pair, which assist complexation as well as extraction of the metal complex into a non-polar solvent. Further, the ion-binding property of a pyrene-armed calix[4]-arene azacrown-5, the ionophore of which is similar to that of the present study, is reported.[30,31] The fluorescence study of this molecule exhibited complexation with K^+, Rb^+, Pb^{2+} and Cu^{2+} with strong to moderate (10^4 to 10^5 M^{-1}) binding constant. We have recently reported the ion-binding property of calix[4]arene azacrown with a $[Ru(bpy)_3]^{2+}$ moiety attached to the nitrogen atom of the azacrown ring and apparently the attached unit does not interact with the encapsulated metal ion.[22] The ion-binding property of these compounds, studied by ^1H NMR spectroscopy, showed complexation with Na^+ and K^+ for the azacrown-5 ionophore and with K^+ and Cs^+ for the azacrown-6 ionophore with moderate binding constant (10^2 to 10^3 M^{-1}). The observation with azacrown-5 is similar to that of compound **1** of the present study. However, compound **3**, which contains a *tert*-butyl group, exhibits complexation with only Na^+ and is due to steric crowding imposed by the *tert*-butyl group, as can be seen in the following section (modeling study).

Modeling studies

The remarkable difference in the selectivity of alkali metal ions with the calix receptors **1** and **3** of similar size prompted us to examine the complexing ability of these systems. Molecular modeling studies were performed for **1** and **3** with sodium and potassium ions. The crystal structure analyses showed that the parent receptors **1–4** are arranged in 1,3-alternate conformations. Having such information in hand, we have modeled the complexations of receptors **1** and **3** with Na^+ and K^+ ions computationally. Solid state structures have been considered as initial guesses in this study.[39] We have employed a molecular mechanics (MMFF94) force field using the Monte Carlo search method to examine the complexations of Na^+ and K^+ ions with **1** and **3** calix receptor molecules. The details of the calculations are mentioned in the computational methodology section. The lowest energy complexed geometries were taken for higher level density functional calculations in a solvent (acetonitrile). The conformational search was performed with the parent crystal structures placing the metal ions near the nitrogen atom connected to the tosyl group, however, pointing away from the calix-crown rings in each case. In general, the *ab initio* and molecular mechanics calculations have been performed with placing the metal ions in the centroid of crowns and calix rings.[40,41] However, we intended to see that during the Monte Carlo searches using the MMFF94 force field, the metal ions reach inside the cavity of the receptors or move away from the confined calix-crown ring. The effect of a counter ion is not present in these calculations. Sodium and potassium ions moved inside the cavity of receptor **1**, whereas, only the sodium ion complexed inside the cavity of receptor **3** (Fig. 7). The *tert*-butyl attached to the phenyl rings present in receptor **3** presumably did not allow the bigger potassium ion to move inside the ring. The binding energies calculated for the complexations of Na^+ and K^+ ions with receptor **1** at the (DFT) GGA/PW91/DNP level in acetonitrile suggest that the potassium ion should be more likely to bind than the sodium ion. Experimental complexations were carried out with mixed solvents (acetonitrile and chloroform), however, in the computational studies the polar solvent acetonitrile was used. The sodium ion being smaller in size moves slightly to the upper side of the azacrown and coordinates with three oxygen atoms. On the other hand, potassium ions bind with 4 oxygen atoms of azacrown rings and the additional stability in the $\mathbf{1}:K^+$ complex compared to $\mathbf{1}:Na^+$ seems to come from the cation–π interactions. The calculated distance between the aryl plane and the potassium ion is 3.2 Å and suggests that cation–π interactions are possible in this case.[42,43] These calculated results corroborate the experimentally observed selectivity pattern.

Calix[4]arene-azacrown-6 receptor **2** is bigger compared to **1** and **3** (Fig. 8). It has been reported that the calix[4]arene-crown-6 can bind larger ions compared to calix[4]arene-crown-4/5

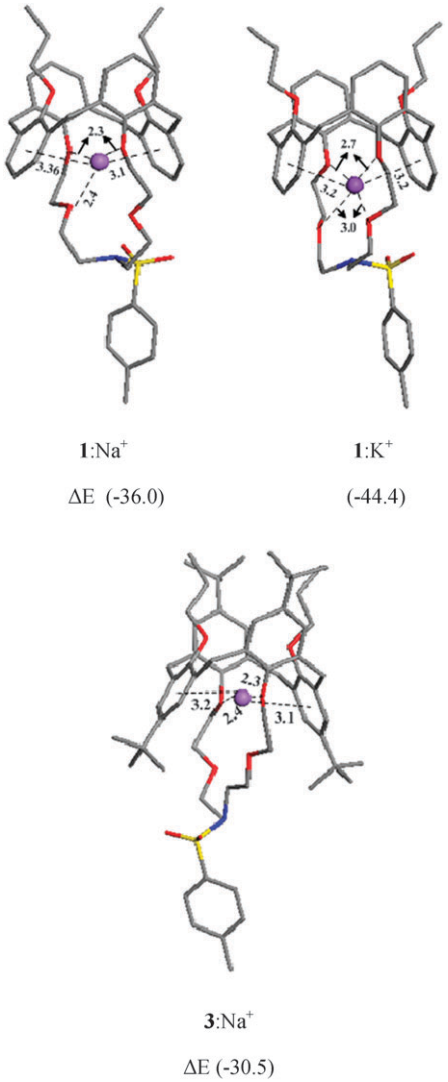

Fig. 7 DFT calculated GGA/PW91/DNP level lowest energy conformations for receptor **1** with Na^+ and K^+; and for **3** with Na^+ (in acetonitrile). Binding energies (ΔE) are in kcal mol^{-1} and the distances are in Å (grey: carbon, red: oxygen, blue: nitrogen, yellow: sulfur).

host molecules.[44] Receptor **2** forms complexes with sodium and potassium ions and in addition binds with rubidium and barium ions also. We have examined the complexation ability of these ions with **2** employing a similar approach with the MMFF94 force field and DFT calculations. The structure of receptor **2** and complexation geometries of **2** with Na^+, K^+, Rb^+, and Ba^{2+} are given in Fig. 8. These metal ions complex inside the cavity of receptor **2** where crown oxygen atoms and the lower rim phenyl rings participate in binding with these metal ions. The calculated binding energies at GGA/PW91/DNP qualitatively corroborate the weaker binding of Na^+ ion with receptor **2**. However, the lower selectivity of the barium ion compared to Rb^+ and K^+ ions was not borne out from these calculated results and such a discrepancy may be ascribed to the fact that the effect of the counter-anion is not taken into account. Calix[4]arene-crown-6 receptors are known to bind Cs^+ ions,[40,44] however, the receptor **2** of

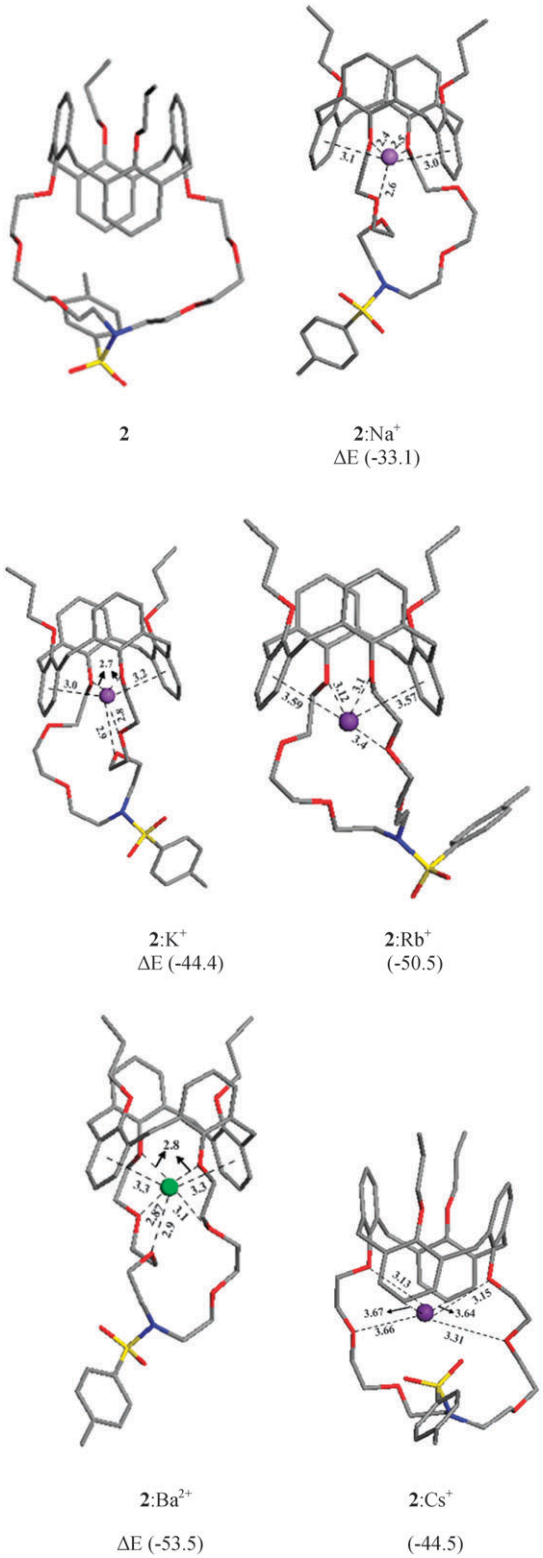

Fig. 8 DFT calculated GGA/PW91/DNP level for the parent structure and the lowest energy conformations for **2** with Na^+, K^+, Rb^+, Ba^{2+} and Cs^+ (in acetonitrile). Binding energies (ΔE) are in kcal mol^{-1} and the distances are in Å (grey: carbon, red: oxygen, blue: nitrogen, yellow: sulfur).

similar size does not seem to complex with the caesium ion, as we have not observed any significant change in ^1H NMR

analysis. Our calculations, however, showed the complexation of the Cs^+ ion with receptor **2** (Fig. 8). The complexation structures show that larger deviations in the lower rim of **2** are seen while complexing with Na^+, K^+, Rb^+ and Ba^{2+} ions compared to the parent elliptical-shape conformation of the azacrown (Fig. 8). The elliptical shape of the azacrown in the Cs^+ ion complex with **2** is less perturbed and presumably not noticeable in NMR spectra.[16] The smallest calix[4]aza-crown-5 having three tosyl substituents did not show complexation with any metal ions studied here. Our modeling studies performed with Na^+ and K^+ ions showed that the metal ions sit at the top of the upper rim of receptor **4**, and not much perturbation was seen in the lower part of **4** with respect to the parent conformation (see Fig. S3 in the ESI†). The complexation energies for Na^+ and K^+ ions were found to be lower with **4** compared to the other receptors. The $-CH_2-$ groups attached to the phenyl rings on the upper side of the azacrown did not deviate greatly while complexing with the metal ions compared to the parent structure and the changes were also not observed in the NMR studies.

Conclusions

A number of calix[4]arene-azacrown receptor molecules with and without a *tert*-butyl group at the upper rim and substituents at the nitrogen atom of the azacrown ring have been synthesized to investigate the effect of steric crowding on ion selectivity. Variation in the crown ring size has also been introduced by incorporating azacrown-5 and azacrown-6 as ionophores. ^{1}H NMR and crystallographic studies have revealed that all of these ionophores exist in a 1,3-alternate conformation in solution and also in the solid state. The cation-binding property of these ionophores with a large number of metal ions has been investigated by ^{1}H NMR, which shows the complexing ability of **1** with Na^+ and K^+, **2** with Na^+, K^+, Rb^+ and Ba^{2+}, **3** with Na^+ and no complexation for **4**. Binding constants for all these metal ions have been determined by ^{1}H NMR titration and the K_s values suggest that steric crowding and size-matching factors have profound influence on ion-selectivity. The difference in the selectivity with cations for **1** and **3** was predicted by molecular modeling studies employing a (MMFF94) force field and DFT calculations. The calculated results also showed that the receptor **2** can bind with Cs^+ and the smaller receptor **4** can bind with Na^+ and K^+ ions on the upper rim, however, such interactions do not perturb the complexation geometries to a larger extent, and presumably such changes are not observable in NMR studies.

Experimental section

General

Elemental analyses (C, H, and N) were performed on a model 2400 Perkin-Elmer elemental analyzer. Mass spectra were recorded on a Q-TOF Micro™ LC-MS instrument. Infrared spectra were recorded on a Perkin-Elmer spectrum GX FT-IR spectrophotometer on KBr pellets. NMR spectra were recorded on models DPX 200 and Avance II 500 Bruker FT-NMR instruments. The UV/Vis spectra were recorded on a model CARY 500 SCAN UV-Vis-NIR spectrophotometer. All the starting materials were purchased either from Sigma Aldrich Company or from S.D. Fine Chemicals. All the perchlorate salts of the cations were purchased from Alfa Aesar (Johnson Matthey Company). Analytical thin-layer chromatography was carried out on silica gel plates (SiO_2, Merck 60 F_{254}) obtained from E. Mark Chemical Co. All organic solvents were analytical grade and used as received for synthesis work and purified by standard procedures for spectroscopic study.[45] The reagents 2-(2-chloroethoxy)-ethanol-*p*-toluenesulfonate,[46] 2-(2-(2-chloroethoxy) ethoxy)-ethanol *p*-toluenesulfonate,[47] *N*,*N*′,*N*′-tritosyldiethylenetriamine,[48] ethanediol ditosyl,[44,48] and the starting compound dipropyloxydihydroxycalix[4]arene (**A** and **B**)[44,48] were prepared following the literature procedures.

Safety note. ***Caution***! Metal perchlorate salts are potentially explosive. So they should be handled with proper care.

Synthesis of the compounds C–F and 1–4

Compounds C and D. The compounds **C** and **D** were prepared following the modified literature procedures[16,22] and the characterization data (NMR and ES-MS) are similar to that reported earlier by us.[22]

Compound E. To a solution of dipropoxydihydroxy-*p*-*tert*-butylcalix[4]arene **B** (1.47 g, 2 mmol), 2-(2-chloroethoxy)-ethanol-*p*-toluenesulfonate (1.11 g, 4 mmol) and Cs_2CO_3 (2.61 g, 8 mmol) in 80 mL of freshly distilled acetonitrile was heated at reflux for 40 h under nitrogen. The reaction mixture was allowed to cool to room temperature and evaporated to dryness by rotary evaporation. To this residue HCl (10%, 100 mL) and CH_2Cl_2 (100 mL) were added and the organic phase was separated and washed twice with water (100 mL each). The organic layer was dried over anhydrous sodium sulfate and evaporated to afford brownish oil. Column chromatography on silica gel (200–400 mesh) with 98 : 2 (v/v) ethyl hexane–ethyl acetate as an eluent provided **E** as white solid. (Yield: 1.30 g, 69%). ^{1}H NMR (500 MHz, CDCl3): δ 7.02 (4H, s, calix-Ar–H), 6.96 (4H, s, calix-Ar–H), 3.83–3.75 (8H, m, ArCH_2Ar), 3.58–3.55 (8H, m, –OCH_2CH_2O–), 3.50 (4H, t, J = 6.75 Hz, –O$CH_2$$CH_2$Cl), 3.34 (4H, t, J = 7.75 Hz, –O$CH_2$$CH_2CH_3$), 3.09 (4H, t, J = 6.75 Hz, –OCH_2CH_2Cl), 1.30 (18H, s, –C(CH_3)$_3$), 1.26 (18H, s, –C(CH_3)$_3$), 1.12–1.08 (4H, m, –$OCH_2CH_2CH_3$), 0.67 (6H, t, J = 7.75 Hz, –$OCH_2CH_2CH_3$). MS, m/z: found 968.54 (100%), Calcd for [**E** + Na^+] 968.50; found 984.53 (40%), Calcd for [**E** + K^+] 984.48. Anal. Calcd for $C_{58}H_{82}Cl_2O_6$: C, 73.61; H, 8.74. Found: C, 73.38; H, 8.52.

Compound F. This compound was prepared following the literature procedure[16] except purification. The compound was purified by column chromatography using silica gel (100–200 mesh) as the column material and ethyl acetate–hexane (1 : 3) as the eluent. The solvent of the desired fraction was evaporated and the mass was dissolved in chloroform (5 mL) and was added to *n*-hexane (40 mL) with stirring. The solid compound thus separated was isolated by filtration and dried in vacuum. Yield: (35%). ^{1}H NMR

(500 MHz, CDCl3): δ 7.83 (4H, d, J = 8.0 Hz, Ar–H of Ts), 7.40 (4H, d, J = 7.5 Hz, Ar–H of Ts), 6.98 (4H, d, J = 7.0 Hz calix-Ar–H), 6.90 (4H, d, J = 7.0 Hz, calix-Ar–H), 6.75 (2H, t, J = 7.25 Hz calix-Ar–H), 6.54 (2H, t, J = 7.0 Hz, calix-Ar–H), 3.81–3.42 (16H, m, 8H for ArCH_2Ar, 8H for –OCH_2CH_2O–), 3.43 (4H J = 7.0 Hz, –OCH_2CH$_2$CH$_3$), 2.48 (6H, s, –CH_3 of Ts), 1.41–1.37 (4H, m, –OCH$_2$$CH_2CH_3$), 0.75 (6H, t, J = 6.75 Hz, –OCH$_2$CH$_2$$CH_3$); MS, m/z: found 927.61 (100%), Calcd for [**F** + Na$^+$] 927.20; found 943.50 (20%), Calcd for [**F** + K$^+$] 943.20. $C_{52}H_{56}O_{10}S_2$: C, 69.02, H, 6.19; found C, 68.97, H, 6.31.

Compounds 1 and 2. These two compounds were prepared following the modified literature procedures[16,22] and the ^{1}H NMR data with assignment of signals (which was not reported earlier) are given here. ^{1}H NMR (500 MHz, $CDCl_3$): for **1**; δ 7.73 (2H, d, J = 8.0 Hz, Ar–H of Ts), 7.40 (2H, d, J = 8.0 Hz, Ar–H of Ts), 7.04 (4H, d, J = 7.5 Hz, calix-Ar–H), 7.02 (4H, d, J = 7.5 Hz, calix-Ar–H), 6.78–6.72 (4H, m, calix-Ar–H), 3.80–3.72 (8H, m, ArCH_2Ar), 3.48 (4H, t, J = 4.75 Hz, –OCH_2CH$_2$O–), 3.41 (4H, t, J = 7.75 Hz, –OCH_2CH$_2$CH$_3$), 3.31–3.24 (12H, m, –OCH_2CH_2N(Ts) and –OCH$_2$$CH_2$O–), 2.45 (3H, s, –$CH_3$), 1.33–1.29 (4H, m, –OCH$_2$$CH_2CH_3$), 0.73 (6H, t, J = 7.5 Hz, –OCH$_2$CH$_2$$CH3$). For **2**; δ 7.73 (2H, d, J = 8.0 Hz, Ar–H of Ts), 7.38 (2H, d, J = 8.0 Hz, Ar–H of Ts), 7.10 (4H, d, J = 7.5 Hz, calix-Ar–H), 7.02 (4H, d, J = 7.5 Hz, calix-Ar–H), 6.76–6.72 (4H, m, calix-Ar–H), 3.71 (8H, m, ArCH_2Ar), 3.64 (4H, t, J = 6.0 Hz, –OCH_2CH$_2$O–), 3.60 (4H, t, J = 5.25 Hz, –OCH$_2$$CH_2$O–), 3.57–3.55 (4H, overlapped triplet, –OCH_2-CH$_2$O–), 3.53–3.51(4H, overlapped triplet, –OCH$_2$$CH_2$O–), 3.47 (4H, t, J = 7.75 Hz, –OCH_2CH$_2$CH$_3$), 3.42 (4H, t, J = 6.0 Hz, –OCH_2CH$_2$N(Ts)), 3.38 (4H, t, J = 5.25 Hz, OCH$_2$$CH_2$N(Ts)), 2.45 (3H, s, –$CH_3$), 1.5–1.46 (4H, m, –OCH$_2$$CH_2CH_3$), 0.81 (6H, t, J = 7.5 Hz, –OCH$_2$CH$_2$$CH_3$).

Compound 3. A solution of **E** (1.89 g, 2 mmol), K_2CO_3 (1.38 g, 10 mmol) and *p*-toluene sulfonamide (0.38 g, 2.2 mmol) in 50 mL of freshly distilled DMF was heated at reflux for 30 h under nitrogen atmosphere. The reaction mixture was allowed to cool to room temperature and DMF was completely removed by rotary evaporation. To this residue 100 mL of 10% aqueous $NaHCO_3$ solution and 150 mL of $CHCl_3$ were added and the organic phase was separated and washed with distilled water 3 times (100 mL each). Finally the organic layer was separated and dried over anhydrous sodium sulfate and evaporated to afford brownish oil. Column chromatography on silica gel (100–200 mesh) with 9 : 1 (v/v) hexane–ethyl acetate as an eluent provided **3** as a white solid, which on recrystallization from acetonitrile gave white crystalline compound **3**. Yield: 1.5 g, (72%). IR (KBr, cm^{-1}) ν 1335 (SO_2), 1120 (SO_2). ^{1}H NMR (500 MHz, $CDCl_3$): δ 7.63 (2H, d, J = 8.0 Hz, Ar–H), 7.30 (2H, d, J = 8.0 Hz, Ar–H), 6.98 (4H, s, calix-Ar–H), 6.96 (4H, s, calix-Ar–H), 3.90–3.82 (8H, m, ArCH_2Ar), 3.40 (4H, t, J = 5.5 Hz, –OCH_2CH$_2$CH$_3$), 3.19–3.16 (8H, m, –CH$_2$OCH$_2$–), 3.14 (4H, t, J = 6.5 Hz, –OCH_2CH$_2$N(Ts)), 2.92 (4H, t, J = 6.5 Hz, –CH_2N(Ts)CH_2–), 2.45 (3H, s, –CH_3), 1.25 (18H, s, –C(CH_3)$_3$), 1.23 (18H, s, –C(CH_3)$_3$), 0.76–0.71 (4H, m, –OCH$_2$$CH_2CH_3$), 0.58 (6H, t, J = 7.5 Hz, –OCH$_2$CH$_2$$CH_3$). MS m/z: found 1066.77 (100%), Calcd for [**3** + Na$^+$] 1066.61. Anal. Calcd for $C_{65}H_{89}NO_8S$: C, 74.74; H, 8.59; N, 1.34; S, 3.06. Found: C, 74.24; H, 8.30; N, 1.32; S, 3.13.

Compound 4. Under nitrogen atmosphere, a solution of **F** (0.45 g, 0.5 mmol), *N*,*N*′,*N*′′-tritosyldiethylenetriamine (0.40 g, 0.7 mmol) and Cs_2CO_3 (0.82 g, 2.5 mmol) in 80 mL of freshly distilled acetonitrile was heated at reflux for 60 h. The reaction mixture was allowed to cool to room temperature and evaporated to dryness by rotary evaporation. To this residue 100 mL of aqueous saturated $NaHCO_3$ solution and 150 mL of CH_2Cl_2 were added. The organic phase was separated and washed twice with distilled water (100 mL each). Finally the organic layer was dried over anhydrous sodium sulfate and evaporated to afford a brownish oil. Column chromatography on silica gel (100–200 mesh) with 7 : 3 (v/v) hexane–ethyl acetate as eluent provided **4** as a white solid. Recrystallization of the crude product from 1 : 1 acetonitrile–chloroform mixture at room temperature gave white crystalline compound **4**. Yield: 0.24 g, (43%). IR (KBr, cm^{-1}) ν 1348 (SO_2), 1159 (SO_2). ^{1}H NMR (500 MHz, $CDCl_3$): δ 7.75 (d, 4H, J = 8.0 Hz, Ar–H of Ts), 7.62 (d, 2H, J = 8.0 Hz, Ar–H of Ts), 7.35 (d, 6H, J = 8.0 Hz, Ar–H, of Ts), 7.0 (d, 4H, J = 7.5 Hz calix-Ar–H), 6.93 (d, 4H, J = 7.5 Hz, calix-Ar–H), 6.8–6.77 (m, 4H, calix-Ar–H), 3.74–3.60 (m, 12H, 8H from ArCH_2Ar and 4H from –OCH_2CH$_2$N–), 3.39 (t, 4H, J = 7.75 Hz, –OCH_2CH$_2$CH$_3$), 3.12 (m, 8H, –OCH$_2$$CH_2$N(Ts)$CH_2CH_2$N–), 2.93 (t, 4H, J = 7.5 Hz, –NCH$_2$$CH_2$N(Ts)–$CH_2CH_2$N–), 2.49 (s, 3H, –$CH_3$), 2.47 (s, 6H, –$CH_3$), 1.31–1.26 (m, 4H, –OCH$_2$$CH_2CH_3$), 0.74 (t, 6H, J = 7.5 Hz, –OCH$_2$CH$_2$$CH_3$). MS m/z: found 1148.84 (100%), Calcd for [**4** + Na$^+$] 1148.41; found 1163.78 (25%), Calcd for [**4** + K$^+$] 1163.39. Anal. Calcd for $C_{63}H_{71}N_3S_3O_{10}$: C, 67.17; H, 6.35; N, 3.73; S, 8.52. Found: C, 66.83; H, 6.56; N, 3.58; S, 8.35.

NMR study

^{1}H NMR spectra of the complexes were recorded with 2 mg of the sample dissolved in 0.5 mL of CD_3CN–$CDCl_3$ (3 : 1). A solid perchlorate salt of desired metal ions (20 equiv.) was added into this solution and the spectra of the resulting mixture were recorded. The spectra of the solutions with cations were compared to those of the original complexes to ascertain the interaction of the metal ions with the ionophore. On the basis of the observation of this study (details are given in the results and discussion section), the interaction of Na$^+$ and K$^+$ for **1**, K$^+$, Rb$^+$ and Ba^{2+} for **2** and Na$^+$ for **3** were chosen to carry out NMR titration.

Stock solutions with desired concentrations of metal (Na$^+$, K$^+$, Rb$^+$, and Ba^{2+}) perchlorate salts were prepared in a CD_3CN–$CDCl_3$ (3 : 1) mixture. ^{1}H NMR spectra of the solutions containing 2 mg of the desired complex dissolved in 0.5 mL of the same solvent mixture were recorded. Into these solutions, required amounts of stock solutions containing metal ions were added by micro syringe to make the concentrations of the cations 0.3 to 15 equivalents of the concentration of the complex and the spectra of the resulting solutions were recorded. In some cases, upon addition of increasing concentrations of metal ion new peaks grew with

the gradual disappearance of the original signals whereas in other cases, a gradual shift of certain signals was noted. In the latter cases, binding constants were calculated using the literature procedure.[37] For the systems where new peaks have grown, the binding constants were determined by a direct method using peak intensity ratio as described in the results and discussion section.[37,38]

Mass spectroscopic study

The formation of a metal complex was also confirmed by mass spectrometry. The ionophores (**1**, **2** and **3**, 0.5 mmol) were dissolved in a CH_3CN–$CHCl_3$ (3 : 1) mixture (30 mL) and desired solid metal perchlorate salts (2.5 mmol) were added into the solutions. The reaction mixtures were stirred at room temperature for 2 h, the solutions were then filtered off and the filtrates were analyzed by a Q-TOF Micro™ LC-MS instrument. The mass data obtained are: MS *m*/*z*: found 859.01 (100%), Calcd for [**1** + K^+] 859.01; found 843.57 (100%), Calcd for [**1** + Na^+] 843.03; found 946.43 (100%), Calcd for [**2** + K^+] 946.39; found 992.20 (100%), Calcd for [**2** + Rb^+] 992.80; found 1044.87 (50%), calcd for [**2** + Ba^{2+}] 1044.46; found 1065.79 (100%), Calcd for [**3** + Na^+] 1065.61.

X-Ray experiments, structure determination and refinements

A crystal of suitable size was selected from the mother liquor and immersed in partone oil, then mounted on the tip of a glass fiber and cemented using epoxy resin. Intensity data for all four crystals were collected at 100 K using graphite monochromatised Mo-Kα (λ = 0.71073 Å) radiation on a Bruker SMART APEX diffractometer equipped with a CCD area detector. The data integration and reduction were processed with SAINT software.[49] An empirical absorption correction was applied to the collected reflections with SADABS.[50] The structures were solved by direct methods using SHELXTL[51] and were refined on F^2 by the full-matrix least-squares technique using the SHELXL-97[52] program package. Graphics are generated using PLATON[53] and MERCURY 1.3.[54] In all the compounds non-hydrogen atoms were refined anisotropically till convergence was reached and the hydrogen atoms attached to the ligand moieties are stereochemically fixed.

Crystal data for 1

$C_{49}H_{57}N_1O_8S_1$; M_r = 820.02; colourless block shaped crystals were grown from diethyl ether. Dimensions of the specimen used for X-ray experiments 0.48 × 0.34 × 0.22 mm. Space group monoclinic $P2_1$. Lattice constants (Å) a = 16.9671(12), b = 10.0972(7), c = 25.6043(19), β (°) = 104.276(2), cell volume V = 4251.1(5) (Å^3), formula units/cell = 4, X-ray density ρ_x = 1.281 g cm^{-3}, $2\theta_{max}$ = 50.0°, number of independent reflections = 7930, reflections collected = 21 383, linear absorption coeff. μ = 13.3 cm^{-1}, R_{int} = 0.0722. After convergence of refinements R_1 = 0.0648, Rw = 0.1264, GoF = 1.076, Flack parameter = 0.17(12).

Crystal data for 2

$C_{53}H_{65}N_1O_{10}S_1$; M_r = 908.12; colourless block shaped crystals were grown from diethyl ether. Dimensions of the specimen used for X-ray experiments 0.56 × 0.38 × 0.25 mm. Space group triclinic $P\bar{1}$. Lattice constants (Å) a = 14.7394(11), b = 17.0425(13), c = 20.6798(16), α = 74.873(3)°, β = 82.029(2)°, γ = 75.019(2)°, cell volume V = 4830.1(6) (Å^3), formula units/cell = 4, X-ray density ρ_x = 1.249 g cm^{-3}, $2\theta_{max}$ = 56.56°. Number of independent reflections 21 770, reflections collected = 41 560, linear absorption coeff. μ = 12.6 cm^{-1}, R_{int} = 0.0232, after convergence of refinements R_1 = 0.0649, Rw = 0.1755, GoF = 1.026.

Crystal data for 3

$C_{65}H_{89}N_1O_8$ S_1; M_r = 1044.43; colourless block shaped crystals were grown from acetonitrile. Dimensions of the specimen used for X-ray experiments 0.40 × 0.20 × 12 mm. Space group monoclinic $P2_1/n$. Lattice constants (Å) a = 15.3737(15), b = 14.3951(15), c = 27.451(3), β = 105.396(2)°, cell volume V = 5857.1(10) (Å^3), formula units/cell = 4, X-ray density ρ_x = 184 g cm^{-3}, $2\theta_{max}$ = 52.0°. Number of independent reflections 11 461, reflections collected = 31 126, linear absorption coeff. μ = 11.0 cm^{-1}, R_{int} = 0.0803, after convergence of refinements R_1 = 0.0953, Rw = 0.1721, GoF = 1.168.

Crystal data for 4

$C_{63}H_{71}N_3O_{10}S_3$; M_r = 1126.41; colourless block shaped crystals were grown from chloroform–acetonitrile (1 : 1). Dimensions of the specimen used for X-ray experiments 0.40 × 0.32 × 0.24 mm. Space group monoclinic $P2_1/c$. Lattice constants (Å) a = 17.422(2), b = 16.931(2), c = 20.781(3), β = 110.187(2)°, cell volume V = 5753.2(13) (Å^3), formula units/cell = 4, X-ray density ρ_x = 1.300 g cm^{-3}, $2\theta_{max}$ = 50.0°. Number of independent reflections 10 100, reflections collected = 28 620, linear absorption coeff. μ = 19.1 cm^{-1}, R_{int} = 0.0803, after convergence of refinements R_1 = 0.0998, Rw = 0.1916, GoF = 1.197.

Computation methodology

Conformational searches were performed using the Monte Carlo algorithm for the random variation of all of the rotatable bonds combined with Merck force field (MMFF94).[55–57] The structural parameters for the receptors, Na^+ and K^+ ions were taken from the inbuilt MMFF94 parameters available in the parameters file. For Ba^{2+} and Rb^+ ions, the parameters were taken from published literature reports.[58] For each calculation, 5000 Monte Carlo steps were carried out. Lowest energy conformers in each case were taken for the energetic comparisons with density functional calculations. DFT calculations were performed with the generalized gradient potential GGA/PW91/DNP level of density functional program Dmol3 in Material Studio (version 4.1) of Accelrys Inc.[59–63] The conductor-like screening model (COSMO) was employed at GGA/PW91/DNP level for solvent (acetonitrile, dielectric = 37.5) calculations.[64,65] The binding energies were computed using the equation, $\Delta E = \Delta E_{complex} - (\Delta E_{ligand} + \Delta E^{M+/2+})$.

Acknowledgements

We are grateful to the Department of Science and Technology (DST), Government of India, for financial support. We thank

CSIR, New Delhi for generous support towards infrastructures and core competency development. S.P. gratefully acknowledges the CSIR for awarding a Senior Research Fellowship (SRF). D.M. and A.S. are thankful to UGC and CSIR New Delhi, India, for awarding a research fellowship (JRF). We thank Mr A. K. Das, Mr V. Agrawal and Mr V. P. Boricha for recording mass, IR and NMR spectra, respectively.

Notes and references

1 C. D. Gutsche, *Calixarenes*, The Royal Society of Chemistry, Cambridge, UK, 1989.
2 V. Böhmer, *Angew. Chem., Int. Ed. Engl.*, 1995, **34**, 713.
3 A. Ikeda and S. Shinkai, *Chem. Rev.*, 1997, **97**, 1713.
4 *Calixarenes in Action*, ed. L. Mandolini and R. Ungaro, Imperical College Press, London, 2000.
5 C. D. Gutsche, *Calixarenenes. An Introduction*, The Royal Society of Chemistry, Cambridge, UK, 2nd edn, 2008.
6 D. Diamond and K. Nolan, *Anal. Chem.*, 2001, **73**, 22A.
7 S. K. Kim, S. H. Lee, J. Y. Lee, J. Y. Lee, R. A. Bartsch and J. S. Kim, *J. Am. Chem. Soc.*, 2004, **126**, 16499.
8 P. K. Lo and M. S. Wong, *Sensors*, 2008, **8**, 5313.
9 B. S. Creaven, D. F. Donlon and J. Mcginley, *Coord. Chem. Rev.*, 2009, **253**, 893.
10 S. E. Matthews, P. Schmitt, V. Felix, M. G. B. Drew and P. D. Beer, *J. Am. Chem. Soc.*, 2002, **124**, 1341.
11 P. R. A. Webber, A. Cowley, M. G. B. Drew and P. D. Beer, *Chem.–Eur. J.*, 2003, **9**, 2439.
12 B. S. Creaven, T. L. Gernon, J. McGinley, A. Moore and H. Toftlund, *Tetrahedron*, 2006, **62**, 9066.
13 G.-K. Li, Z.-X. Xu, C.-F. Chen and Z.-T. Huang, *Chem. Commun.*, 2008, 1774.
14 R. Joseph, B. Ramanujam, A. Achariya, A. Khutia and C. P. Rao, *J. Org. Chem.*, 2008, **73**, 5745.
15 E. Ghidini, F. Ugozzoli, R. Ungaro, S. Harkema, A. A. El-Fadl and D. N. Reinhoudt, *J. Am. Chem. Soc.*, 1990, **112**, 6979.
16 J. S. Kim, O. J. Shon, J. W. Ko, M. H. Cho, I. Y. Yu and J. Vicens, *J. Org. Chem.*, 2000, **65**, 2386.
17 A. Casnati, N. C. Della, F. Sansone, F. Ugozzoli and R. Ungaro, *Tetrahedron*, 2004, **60**, 7869.
18 H. Zhou, K. Surowiec, D. W. Purkiss and R. A. Bartsch, *Org. Biomol. Chem.*, 2005, **3**, 1676.
19 M. Yuan, W. Zhou, X. Liu, M. Zhu, J. Li, X. Yin, H. Zheng, Z. Zuo, C. Ouyang, H. Liu, Y. Li and D. Zhu, *J. Org. Chem.*, 2008, **73**, 5008.
20 X. Liu, K. Surowiec and R. A. Bartsch, *Tetrahedron*, 2009, **65**, 5893.
21 P. Agnihotri, E. Suresh, P. Paul and P. K. Ghosh, *Eur. J. Inorg. Chem.*, 2006, 3369.
22 S. Patra and P. Paul, *Dalton Trans.*, 2009, 8683.
23 K. Iwamoto, K. Araki and S. Shinkai, *Tetrahedron*, 1991, **47**, 4325.
24 A. Ikeda and S. Shinkai, *J. Am. Chem. Soc.*, 1994, **116**, 3102.
25 S. Patra, E. Suresh and P. Paul, *Polyhedron*, 2007, **26**, 4971.
26 H. M. Chawla, S. N. Sahu and R. Shrivastava, *Tetrahedron Lett.*, 2007, **48**, 6054.
27 J. N. Babu, V. Bhalla, M. Kumar, R. K. Puri and R. K. Mahajan, *New J. Chem.*, 2009, **33**, 675.
28 H. M. Chawla, S. P. Singh and S. Upreti, *Tetrahedron*, 2007, **63**, 5636.
29 J. S. Kim, O. J. Shon, W. Sim, S. K. Kim, M. H. Cho, J.-G. Kim, II.-H. Suh and D. W. Kim, *J. Chem. Soc., Perkin Trans. 1*, 2001, 31.
30 J. S. Kim, O. J. Shon, J. A. Rim, S. K. Kim and J. Yoon, *J. Org. Chem.*, 2002, **67**, 2348.
31 J. S. Kim, K. H. Noh, S. H. Lee, S. K. Kim, S. K. Kim and J. Yoon, *J. Org. Chem.*, 2003, **68**, 597.
32 J.-P. Malval, I. Leray and B. Valeur, *New J. Chem.*, 2005, **29**, 1089.
33 V. P. Boricha, S. Patra, Y. S. Chouhan, P. Sanavada, E. Suresh and P. Paul, *Eur. J. Inorg. Chem.*, 2009, 1256.
34 A. Jaiyu, R. Rojanathanes and M. Sukwattanasinitt, *Tetrahedron Lett.*, 2007, **48**, 1817.
35 P. D. J. Grootenhuis, P. A. Kollman, L. C. Groenen, D. N. Reinhoudt, G. J. V. Hummel, F. Ugozzoli and G. D. Andreeti, *J. Am. Chem. Soc.*, 1990, **112**, 4165.
36 T. Harada, F. Ohseto and S. Shinkai, *Tetrahedron*, 1994, **50**, 13377.
37 K. Hirose, *J. Inclusion Phenom. Macrocyclic Chem.*, 2001, **39**, 193.
38 K. N. Koh, K. Araki, S. Shinkai, Z. Asfari and J. Vicens, *Tetrahedron Lett.*, 1995, **36**, 6095.
39 P. D. J. Grootenhuis and P. Kollman, *J. Am. Chem. Soc.*, 1989, **111**, 2152.
40 A. Casnati, D. N. Ca', F. Sansone, F. Ugozzoli and R. Ungaro, *Tetrahedron*, 2004, **60**, 7869.
41 P. Agnihotri, E. Suresh, B. Ganguly, P. Paul and P. K. Ghosh, *Polyhedron*, 2005, **24**, 1023.
42 A. T. Macias, E. N. Joseph and J. D. Evanseck, *J. Am. Chem. Soc.*, 2003, **125**, 2351.
43 J. Cioslowski and Q. Lint, *J. Am. Chem. Soc.*, 1995, **117**, 2553.
44 A. Casnati, A. Pochini, R. Ungaro, F. Ugozzoli, F. Arnaud, S. Fanni, M.-J. Schwing, R. J. M. Egberink, F. de Jong and D. N. Reinhoudt, *J. Am. Chem. Soc.*, 1995, **117**, 2767.
45 D. D. Perrin, W. L. F. Armarego and D. R. Perrin, *Purification of Laboratory Chemicals*, Pergamon Press, Oxford, 2nd edn, 1980.
46 M. Ouchi, Y. Inoue, T. Kanzaki and T. Hakushi, *J. Org. Chem.*, 1984, **49**, 1408.
47 R. W. Hay and P. R. Norman, *J. Chem. Soc., Dalton Trans.*, 1979, 1441.
48 D. W. White, B. A. Karcher, R. A. Jabcoson and J. G. Verkade, *J. Am. Chem. Soc.*, 1979, **101**, 4921.
49 G. M. Sheldrick, SAINT 5.1 ed., Siemens Industrial Automation Inc., Madison, WI, 1995.
50 SADABS, Empirical Absorption Correction Program;University of Göttingen, Göttingen, Germany, 1997.
51 G. M. Sheldrick, *SHELXTL Reference Manual: Version 5.1*, Bruker AXS, Madison, WI, 1997.
52 G. M. Sheldrick, *SHELXL-97: Program for Crystal Structure Refinement*, University of Göttingen, Göttingen, Germany, 1997.
53 A. L. Spek, *PLATON-97*, University of Utrecht, Utrecht The Netherlands, 1997.
54 Mercury 1.3, Supplied with Cambridge Structural Database; CCDC: Cambridge, U.K., 2003.
55 Spartan'06, Wavefunction Inc.: Irvine, California.
56 T. A. Halgren, *J. Comput. Chem.*, 1996, **17**, 490.
57 W. J. Hehre, *A Guide to Molecular Mechanics and Quantum Chemical Calculations*, Wavefuncton Inc., Irvine, CA, 2nd edn, 2006.
58 H. Coker, *J. Phys. Chem.*, 1976, **80**, 2078.
59 B. J. Delley, *Chem. Phys.*, 2000, **113**, 7756–7763.
60 J. P. Perdew and Y. Wang, *Phys. Rev. B: Condens. Matter*, 1992, **45**, 13244–13249.
61 Z. Wu, R. E. Cohen and D. Singh, *Phys. Rev. B: Condens. Matter Mater. Phys.*, 2004, **70**, 104112.
62 J. P. Perdew, K. Burke and Y. Wang, *Phys. Rev. B: Condens. Matter*, 1996, **54**, 16533–16539.
63 Materials Studio DMOL3 Version 4.1, Accelrys Inc., San Diego, USA.
64 A. Klamt, COSMO and COSMO-RS, in *Encyclopedia of Computational Chemistry*, ed. P. v. R. Schleyer and L. Allinger, Wiley, New York, 1998, vol. 2, pp. 604–615.
65 A. Klamt, *J. Phys. Chem.*, 1995, **99**, 2224–2235.